Science Advances

AAAS

advances.sciencemag.org/cgi/content/full/2/4/e1500887/DC1

Supplementary Materials for

Bioengineering a 3D integumentary organ system from iPS cells using an in vivo transplantation model

Ryoji Takagi, Junko Ishimaru, Ayaka Sugawara, Koh-ei Toyoshima, Kentaro Ishida, Miho Ogawa, Kei Sakakibara, Kyosuke Asakawa, Akitoshi Kashiwakura, Masamitsu Oshima, Ryohei Minamide, Akio Sato, Toshihiro Yoshitake, Akira Takeda, Hiroshi Egusa, Takashi Tsuji

Published 1 April 2016, *Sci. Adv.* **2**, e1500887 (2016)
DOI: 10.1126/sciadv.1500887

The PDF file includes:

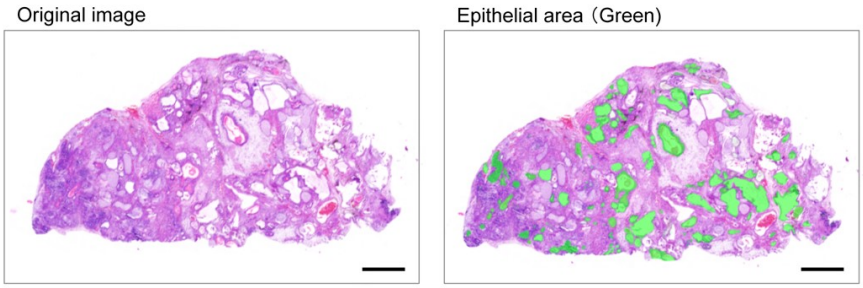

fig. S1. Analysis of the area of the cystic lumen. The measurement area of the cystic in explants are shown by green area using image analysis software, such as Image J. Original data (left) and measured data (right) are shown. Scale bars, 1 mm.

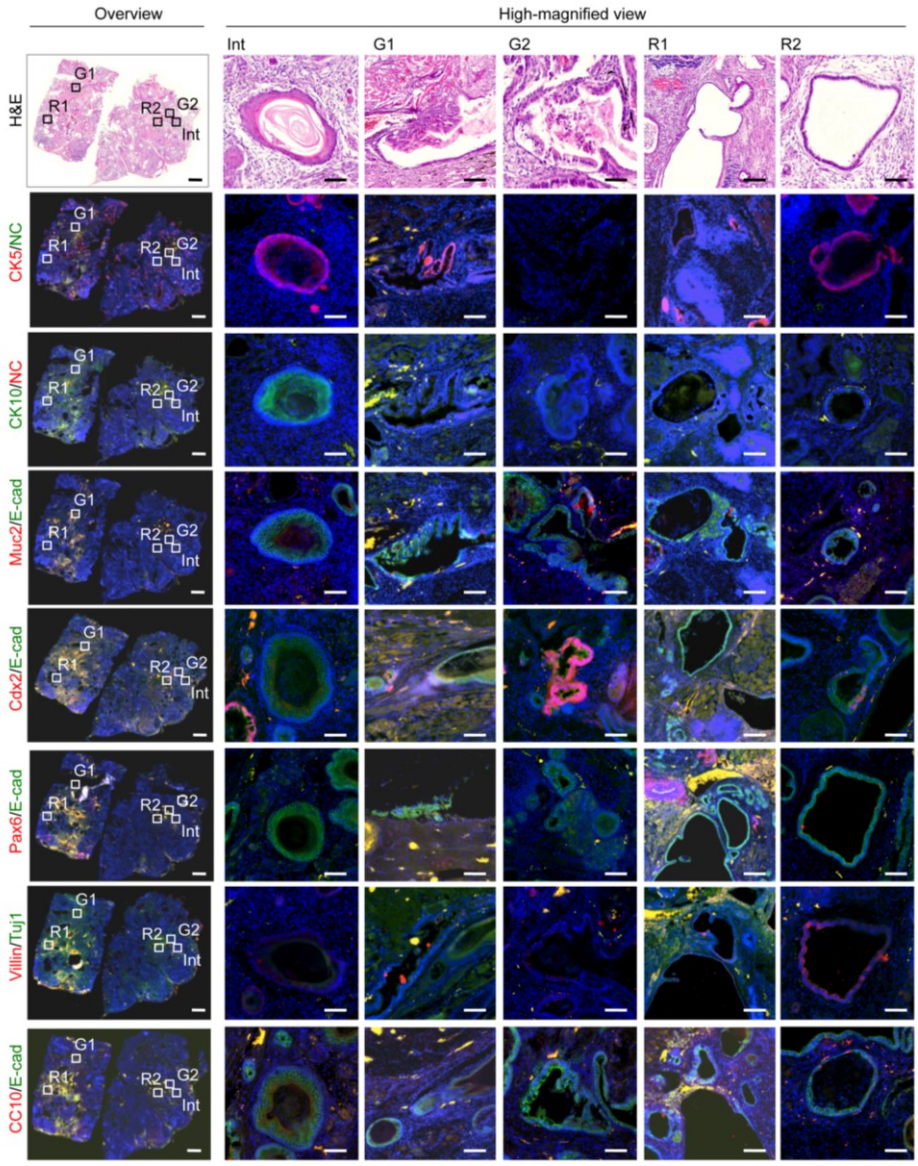

fig. S2. Histochemical and immunohistochemical analyses of the cystic epithelia in the in vivo explants of multiple iPS cell–derived EBs. Boxed areas in the upper left panel (H&E staining) are shown at higher magnification in the upper right panels. To identify the epithelial types, such as ectodermal epithelium, integument (Int), and endodermal epithelium such as respiratory tract (R1 and R2) and gastrointestinal tube (G1 and G2), the CDB transplants were analysed by immunostaining with specific antibodies for CK5, CK10, Muc2, Cdx2, Pax6, Villin, CC10, Tuj1 and E-cadherin. The nuclei were stained using Hoechst 33258 (nuc, blue). Scale bars, 1 mm in overviews, 100 μm in high-magnified images.

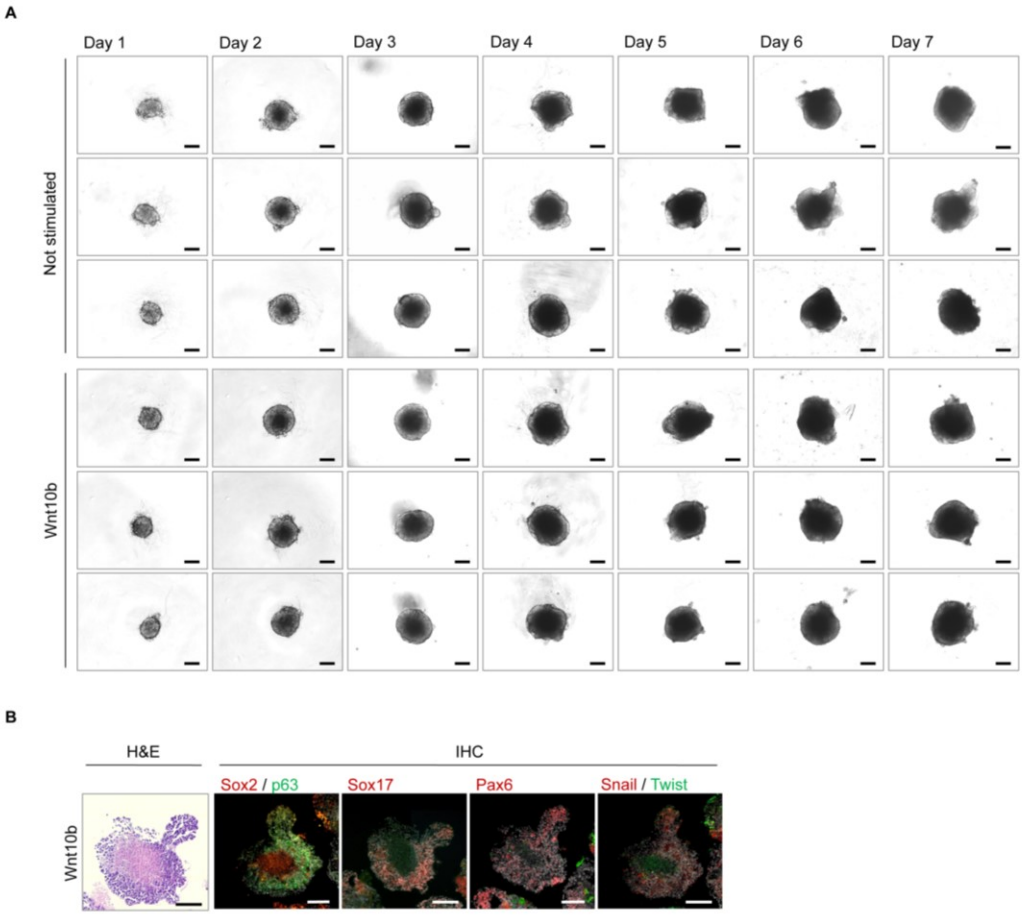

fig. S3. Culture of iPS cells for EB formation. A. Phase-contrast images of iPS cells and the formation of EBs, which were cultured in non-adherent plastic wells for 1 to 7 days. The photographs of EBs show each three independent EBs were stimulated without (upper panels) or with Wnt10b (lower panels). Scale bars, 100 μm. **B.** H&E staining and immunostaining of EBs, using antibodies to epithelial (Sox2, p63, and Sox17), neural progenitor marker (Pax6) and neural crest markers (Snail and Twist) after 7 days in EB culture with Wnt10b. The nuclei were stained using Hoechst 33258 (white). Scale bars, 50 μm.

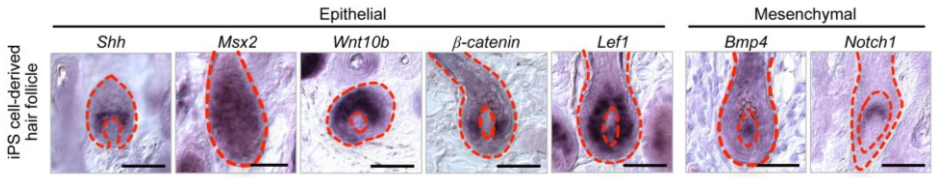

fig. S4. Gene expression in iPS cell–derived bioengineered hair follicle germs in a 3D IOS generated via the CDB transplantation method. Expressions of regulatory genes during hair follicle development in bioengineered hair follicle germs are shown. Gene expression was detected by in situ hybridization. Dotted lines indicate the interface between the epithelial and mesenchymal cells. The hair germ epithelial markers *Shh, Msx2, Wnt10b, β-catenin* and *Lef1* and mesenchymal markers *Bmp4* and *Notch1* were detected iPS cell-derived bioengineered hair follicle germs. Scale bars, 50 μm.

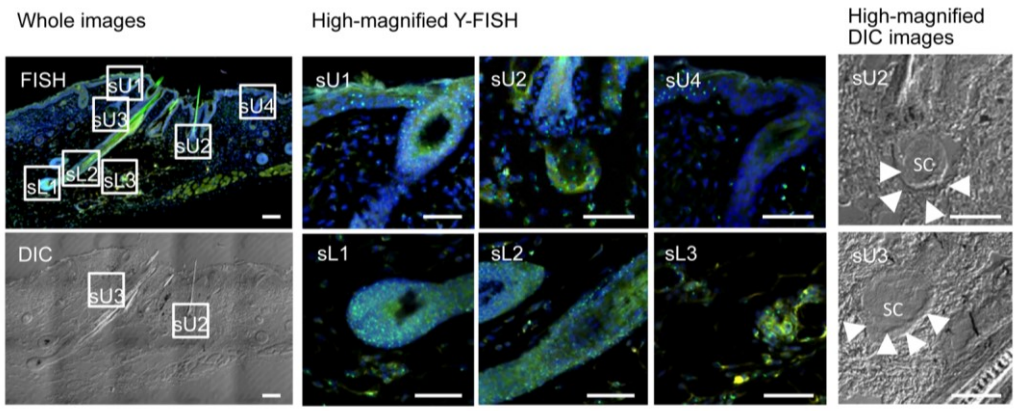

fig. S5. Y-FISH analysis of distribution of iPS cell–derived cells among the 3D IOSs grafted to the natural murine skin. Y-chromosome FISH analysis of the MEB transplants using male mouse-specific DNA probes. These images are obtained from a serial section, which are shown in Fig. 3C. Whole Y-FISH and DIC images of grafted area are shown in the left panels. FISH images are shown in the left upper panel. Green and blue signals indicate Y-chromosome-positive cells and nuclei, respectively. Boxed areas in the FISH image are shown at a higher magnification in the center panels. Boxed areas of whole DIC images are shown at a higher magnification in the right panels. FISH images of sU3 region are shown in Fig 3C. Boxed area, sU1, sU2, sU3 and sU4 indicated the skin epithelium and upper region of hair follicle. Especially, boxed area, sU2 and sU3 indicate sebaceous gland. Boxed area, sL1 and sL2, indicate the lower hair bulb region. Boxed sL3 indicates intracutaneous adipose tissue. Arrow heads and SC in the high-magnified DIC images indicate peripheral cells and sebocyte of sebaceous gland, respectively. Scale bars, 200 μm in whole images and 100 μm in high-magnified images.

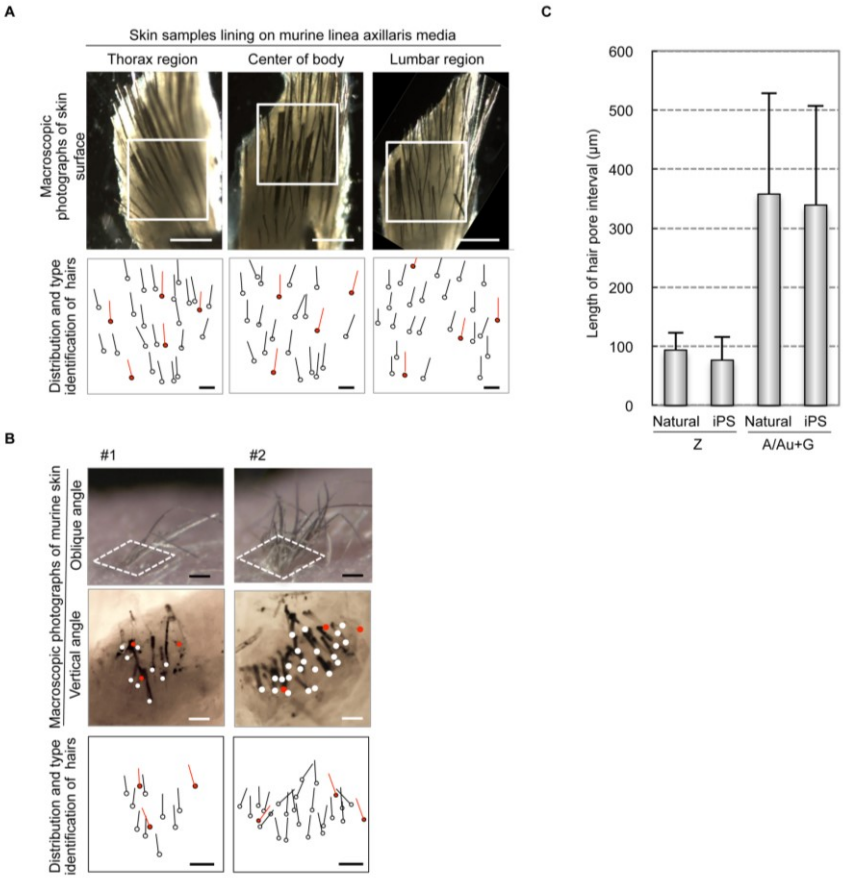

fig. S6. Distribution of hair species of iPS cell–derived hairs. A. Distribution of the murine pelage in the three different regions (thorax, body center and lumbar regions) of side trunk skin lining on murine linea axillaris media. Dissected skin samples were fixed and placed horizontally on a plastic dish before macroscopic photographs. Position of hair pores (white or red dots in the lower) in the 1 mm^2 range (white square in the upper photographs), hair growth direction (black or red bars) and types of hair shaft, which were classified zigzag type (white dots） and awl/auchene and guard type (red dots), were evaluated and represented in the lower charts. Scale bars, 500 μm in upper macroscopic images, and 100 μm in the lower charts. **B**. Distribution of hair species of the iPS cell-derived whole skin transplantation portions. Typical two samples are displayed in this figure. Transplantation sites with iPS cell-derived hairs under the condition of hair growing phase (anagen VI) were identified by oblique angle macroscopic observation (upper). Surgically resected skins were placed horizontally on a plastic dish and before vertical angle macroscopic photographs after hair shaft sampling (middle). Position of

iPS cell-derived hair pores (white or red dots in the lower) in the range of 1 mm^2 FUT portions (white dotted square in the upper photographs), hair growth direction (black or red bars) and types of hair shaft, which were classified zigzag type (white dots) and awl/auchene and guard type (red dots), are represented in the charts (lower). Scale bars, 500 μm in upper macroscopic images, and 100 μm in the lower charts. **C**. Comparison of distance of hair pores with two types of hair shafts including zigzag (Z), awl/auchene (A/Au) and guard (G) on natural mice and iPS cell-derived skin transplantation sites. The data are presented as the mean ± s.e.m. from four individual iPS cell-derived FUT sites and three natural skin (interval length of zigzag hairs, n=17 in natural skin and n=61 in iPS cell-derived skin transplantation sites; awl/auchene and guard hairs, n=12 and n=9 in natural skin and iPS cell-derived skin transplantation sites).

Table S1. Primer sequences used in real-time PCR.

Gene	Forward primer	Reverse Primer
mNanog	TCTGGGAACGCCTCATCAATGCC	GCAGGTCTTCAGAGGAAGGGCG
mOct4	AGGTGGAACCAACTCCCGAGG	GAGAACGCCCAGGGTGAGCC
mNestin	GGCAGCAACTGGCACACCTCA	TGCAGCTTCAGCTTGGGGTCAG
mTrp63	TCCCAGCAGGGTGTCACGCT	GCTCAGAGGGAGCTCGAGGCT
mSox10	CAGTACCCTCACCTCCACAATG	GCGCTTGTCACTTTCGTTCA
mPax3	CAAGCTGGAGCCAATCAACTG	GCGGTGGGAGGGAATCC
m-beta-actin	TGACAGGATGCAGAAGGAGA	GCTGGAAGGTGGACAGTGAG